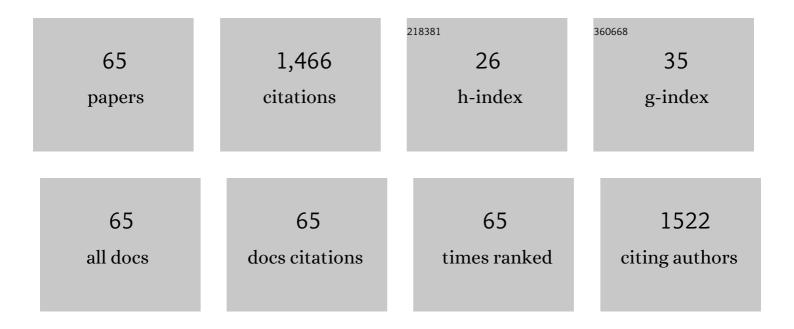
List of Publications by Year in descending order

Source: https://exaly.com/author-pdf/5294413/publications.pdf Version: 2024-02-01



LIVE FANC

#	Article	IF	CITATIONS
1	Liquid-crystalline ordering of davydov-split aggregates of cyanine dyes. Colloids and Surfaces A: Physicochemical and Engineering Aspects, 2022, 642, 128713.	2.3	2
2	Targeting the resolution pathway of inflammation using Ac2–26 peptide-loaded PECylated lipid nanoparticles for the remission of rheumatoid arthritis. Asian Journal of Pharmaceutical Sciences, 2021, 16, 483-493.	4.3	10
3	Dual-Stimuli Responsive Polymeric Micelles for the Effective Treatment of Rheumatoid Arthritis. ACS Applied Materials & Interfaces, 2021, 13, 21076-21086.	4.0	40
4	Nanomedicines for the treatment of rheumatoid arthritis: State of art and potential therapeutic strategies. Acta Pharmaceutica Sinica B, 2021, 11, 1158-1174.	5.7	55
5	Fluorescent H-Aggregate Vesicles and Tubes of a Cyanine Dye and Their Potential as Light-Harvesting Antennae. Journal of Physical Chemistry B, 2021, 125, 7911-7918.	1.2	7
6	Injectable Micelle-Incorporated Hydrogels for the Localized Chemo-Immunotherapy of Breast Tumors. ACS Applied Materials & Interfaces, 2021, 13, 46270-46281.	4.0	11
7	Colorimetric Detection of Dopamine with J-Aggregate Nanotube-Integrated Hydrogel Thin Films. ACS Omega, 2020, 5, 18198-18204.	1.6	14
8	PLA <sub>2</sub> -Triggered Release of Drugs from Self-Assembled Lipid Tubules for Arthritis Treatments. ACS Applied Bio Materials, 2020, 3, 6488-6496.	2.3	12
9	Davydov Split Aggregates of Cyanine Dyes on Self-Assembled Nanotubes. Langmuir, 2020, 36, 13649-13655.	1.6	7
10	Transition from H-Aggregate Nanotubes to J-Aggregate Nanoribbons. Journal of Physical Chemistry C, 2020, 124, 11722-11729.	1.5	8
11	Matrix Metalloproteinase-Responsive PEGylated Lipid Nanoparticles for Controlled Drug Delivery in the Treatment of Rheumatoid Arthritis. ACS Applied Bio Materials, 2020, 3, 3276-3284.	2.3	27
12	Improving the anti-inflammatory efficacy of dexamethasone in the treatment of rheumatoid arthritis with polymerized stealth liposomes as a delivery vehicle. Journal of Materials Chemistry B, 2020, 8, 1841-1851.	2.9	41
13	Morphology Transformation of Supramolecular Structures in Aqueous Mixtures of Two Oppositely Charged Amphiphiles. Langmuir, 2019, 35, 9004-9010.	1.6	4
14	Influence of polymer networks on the sensor properties of hydrogel dispersed liquid crystal droplets. Colloids and Surfaces A: Physicochemical and Engineering Aspects, 2019, 570, 438-443.	2.3	8
15	The formation of ultrafine polyamide 6 nanofiber membranes with needleless electrospinning for air filtration. Polymers for Advanced Technologies, 2019, 30, 1635-1643.	1.6	27
16	Surface modified liquid crystal droplets as an optical probe for the detection of bile acids in microfluidic channels. Colloids and Surfaces A: Physicochemical and Engineering Aspects, 2018, 542, 52-58.	2.3	16
17	Preparation of multi-layer nylon-6 nanofibrous membranes by electrospinning and hot pressing methods for dye filtration. RSC Advances, 2018, 8, 12173-12178.	1.7	26
18	Soft-Templated Synthesis of Lightweight, Elastic, and Conductive Nanotube Aerogels. ACS Applied Materials & Interfaces, 2018, 10, 37426-37433.	4.0	16

#	Article	IF	CITATIONS
19	Mechanical and thermal conductive properties of fiberâ€reinforced silicaâ€alumina aerogels. International Journal of Applied Ceramic Technology, 2018, 15, 1138-1145.	1.1	29
20	Structure and thermal properties of millimeter-scale alumina aerogel beads formed by a modified ball dropping method. RSC Advances, 2017, 7, 1540-1545.	1.7	9
21	Characterizing Viscoelastic Modulations in Biopolymer Hydrogels by Coherence-Gated Light Scattering. Journal of Physical Chemistry B, 2017, 121, 9234-9238.	1.2	4
22	Formation of Spherulitic J-Aggregates from the Coassembly of Lithocholic Acid and Cyanine Dye. Journal of Physical Chemistry Letters, 2017, 8, 4504-4509.	2.1	11
23	Electrical conductivity of silicon carbonitrideâ€reduced graphene oxide composites. Journal of the American Ceramic Society, 2017, 100, 5113-5119.	1.9	14
24	Si <scp>CNO</scp> – <scp>GO</scp> composites with the negative temperature coefficient of resistance for highâ€temperature sensor applications. Journal of the American Ceramic Society, 2017, 100, 592-601.	1.9	33
25	Novel Microstructured Si <scp>CNO</scp> Films Based on Polyvinylsilazaneâ€&welled F127 Micelles. Journal of the American Ceramic Society, 2016, 99, 723-726.	1.9	2
26	Liquid Crystal Droplet-Embedded Biopolymer Hydrogel Sheets for Biosensor Applications. ACS Applied Materials & Interfaces, 2016, 8, 3928-3932.	4.0	67
27	12.4: A Liquid Crystal Biosensor for Liver Diseases. Digest of Technical Papers SID International Symposium, 2015, 46, 147-150.	0.1	1
28	Formation of Novel Microstructured Si <scp>CNO</scp> Films from Block Copolymer Micellarâ€Templating Approaches. Journal of the American Ceramic Society, 2015, 98, 2894-2901.	1.9	6
29	A Facile and Fast Gelation Process to Prepare Highly Spherical Millimeter‧ized Silica Aerogel Beads. International Journal of Applied Ceramic Technology, 2015, 12, E244.	1.1	3
30	Effect of Thermal Initiator Concentrations on the Structure and Optical Band Gaps of Polyvinylsilazaneâ€Đerived SiOCN Ceramics. International Journal of Applied Ceramic Technology, 2015, 12, 985-990.	1.1	3
31	Design of β-CD–surfactant complex-coated liquid crystal droplets for the detection of cholic acid via competitive host–guest recognition. Chemical Communications, 2015, 51, 8912-8915.	2.2	29
32	Synthesis of silica aerogel microspheres by a two-step acid–base sol–gel reaction with emulsification technique. Journal of Porous Materials, 2015, 22, 621-628.	1.3	19
33	Superhydrophobic and superoleophilic "sponge-like―aerogels for oil/water separation. Journal of Materials Science, 2015, 50, 5115-5124.	1.7	40
34	Synthesis of silica–titania composite aerogel beads for the removal of Rhodamine B in water. RSC Advances, 2015, 5, 72437-72443.	1.7	39
35	Tailoring the surface of liquid crystal droplets with chitosan/surfactant complexes for the selective detection of bile acids in biological fluids. RSC Advances, 2015, 5, 70094-70100.	1.7	11
36	A Facile Route to Construct <scp>S</scp> i <scp>CO</scp> Nanospheres with Tunable Sizes. International Journal of Applied Ceramic Technology, 2014, 11, 670-675.	1.1	0

#	Article	IF	CITATIONS
37	Self-Assembly of J-Aggregate Nanotubes and Their Applications for Sensing Dopamine. Langmuir, 2014, 30, 805-811.	1.6	47
38	Protein-Induced Configuration Transitions of Polyelectrolyte-Modified Liquid Crystal Droplets. Journal of Physical Chemistry B, 2014, 118, 4970-4975.	1.2	44
39	Preparation of flexible, hydrophobic, and oleophilic silica aerogels based on a methyltriethoxysilane precursor. Journal of Materials Science, 2014, 49, 7715-7722.	1.7	44
40	Bile acid–surfactant interactions at the liquid crystal/aqueous interface. Soft Matter, 2014, 10, 4609.	1.2	16
41	Liquid crystal based sensors for the detection of cholic acid. Analytical Methods, 2013, 5, 4126.	1.3	28
42	Self-assembled palladium–organic composite nanofibers and their applications as a recyclable catalyst. RSC Advances, 2013, 3, 21576.	1.7	3
43	Optical Detection of Lithocholic Acid with Liquid Crystal Emulsions. Langmuir, 2013, 29, 387-392.	1.6	40
44	Polyelectrolyte-coated liquid crystal droplets for detecting charged macromolecules. Journal of Materials Chemistry, 2012, 22, 6807.	6.7	48
45	Transcription of pH-sensitive supramolecular assemblies into silica: from straight, coiled, and helical tubes to single and double fan-like bundles. Journal of Materials Chemistry, 2011, 21, 13973.	6.7	7
46	Adhesive polymer-dispersed liquid crystal films. Journal of Materials Chemistry, 2011, 21, 9149.	6.7	22
47	Longitudinal Zipping/Unzipping of Self-Assembled Organic Tubes. Journal of Physical Chemistry B, 2011, 115, 14445-14449.	1.2	31
48	Synthesis of nanostructured silicon carbide at ultralow temperature using self-assembled polymer micelles as a precursor. Journal of Materials Chemistry, 2011, 21, 17619.	6.7	9
49	Synthesis of Spherical Nonâ€Oxide Silicon Carbonitride Ceramic Particles. Journal of the American Ceramic Society, 2011, 94, 2779-2782.	1.9	17
50	Selfâ€Assembly of pH‧witchable Spiral Tubes: Supramolecular Chemical Springs. Small, 2010, 6, 217-220.	5.2	67
51	Director Configuration of Liquid-Crystal Droplets Encapsulated by Polyelectrolytes. Langmuir, 2010, 26, 7025-7028.	1.6	30
52	Fluorescent composite tubes with pH-controlled shapes. Journal of Materials Chemistry, 2010, 20, 3716.	6.7	16
53	Assembly of vesicles into fractal and prong patterns on substrates. Soft Matter, 2010, 6, 2139.	1.2	6
54	Assembly and disassembly of tubular spherulites. Soft Matter, 2010, 6, 1224.	1.2	26

#	Article	IF	CITATIONS
55	Radial Elasticity of Self-Assembled Lipid Tubules. ACS Nano, 2008, 2, 1466-1472.	7.3	19
56	Ordered arrays of self-assembled lipid tubules: fabrication and applications. Journal of Materials Chemistry, 2007, 17, 3479.	6.7	51
57	Heterogeneous and Anomalous Diffusion inside Lipid Tubules. Journal of Physical Chemistry B, 2007, 111, 14244-14249.	1.2	40
58	Positioning and Alignment of Lipid Tubules on Patterned Au Substrates. Langmuir, 2006, 22, 1891-1895.	1.6	22
59	Nanoscale Ripples in Self-Assembled Lipid Tubules. Langmuir, 2006, 22, 1973-1975.	1.6	19
60	IPS-LCD Using a Glass Substrate and an Anisotropic Polymer Film. Journal of Display Technology, 2006, 2, 21-25.	1.3	33
61	Self-Assembled Cylindrical Lipid Tubules with a Birefringent Core. Small, 2006, 2, 364-367.	5.2	30
62	Polarization-independent liquid crystal phase modulator with a large phase shift and low operating voltage. , 2006, , .		0
63	Liquid-crystal imaging of molecular-tilt ordering in self-assembled lipid tubules. Proceedings of the National Academy of Sciences of the United States of America, 2005, 102, 7438-7442.	3.3	44
64	Patterning Polymerized Lipid Vesicles with Soft Lithography. Langmuir, 2005, 21, 3132-3135.	1.6	18
65	Imaging the Azimuthal Tilt Order in Monolayers by Liquid Crystal Optical Amplification. Langmuir, 1999, 15, 297-299.	1.6	38